# Nanocomposite Particles with Core-Shell Morphology. I. Preparation and Characterization of $Fe_3O_4$–Poly(butyl acrylate-styrene) Particles via Miniemulsion Polymerization

**Ali Reza Mahdavian, Mohsen Ashjari, Hamid Salehi Mobarakeh**

*Polymer Science Department, Iran Polymer and Petrochemical Institute, Tehran, Iran*

Received 12 September 2007; accepted 3 May 2008
DOI 10.1002/app.28729
Published online 11 July 2008 in Wiley InterScience (www.interscience.wiley.com).

**ABSTRACT:** Colloidal particles with magnetic properties have become increasingly important both technologically and for fundamental studies. Here, chemical initiator-free miniemulsion polymerization of styrene and butyl acrylate has been performed for preparation of magnetic nanocomposite particles with the diameter of 81–150 nm in the presence of sodium dodecyl sulfate as surfactant, span 80 as stabilizer, and hexadecane as hydrophobe. The polymerization reaction was initiated and progressed under ultrasonic irradiation, generated by immersed probe into the latex. The key point in achievement of encapsulation of modified $Fe_3O_4$ nanoparticles was preparation of a stable colloidal dispersion at the end of the reaction. The obtained products in each step were characterized by FTIR spectroscopy. Dynamic light scattering analysis was used to follow particle size diameter of the samples. Morphology of the particles and formation of core-shell structure were analyzed by SEM and TEM micrographs, respectively. TGA and magnetometry of the polymeric films confirmed the extent of insertion of used magnetite and their corresponding behavior. © 2008 Wiley Periodicals, Inc. J Appl Polym Sci 110: 1242–1249, 2008

**Key words:** nanocomposite particle; miniemulsion polymerization; $Fe_3O_4$ nanoparticle; ultrasonic; encapsulation

## INTRODUCTION

Currently, major efforts have been devoted to the controlled formation and application of nanoparticle compounds of polymeric and inorganic materials with core-shell morphology in science and technology. Magnetite nanoparticles homogeneously encapsulated in a hydrophobic polymer, which keep water-soluble components away from contacting the magnetite particles, are of high interest.[1,2] The main advantage of magnetic nanocomposite particles (MCPs) over conventional polymer nanocomposite particles is that, because of their magnetic properties, they can be rapidly separated from the mixtures by magnetic extraction.[3] They have been tried extensively in various fields, such as cell separation,[4] protein purification,[5] environment and food analysis,[6] organic and biochemical synthesis,[7] and industrial water treatment.[8] The MCPs are also used for magnetic ion-exchange resins to purify contaminated water.[9] To date, they are in use, for example, as magnetically controlled seals and bearings, and as loudspeaker coolings.[10] A number of strategies for the preparation of the MCPs have been used to encapsulate magnetic nanoparticles inside polymers by various polymerization methods, including conventional emulsion polymerization,[11] soapless emulsion polymerization,[12] inverse emulsion polymerization,[13] inverse microemulsion polymerization,[14] suspension polymerization,[9] miniemulsion polymerization,[15] dispersion polymerization,[16] seed precipitation polymerization,[17] and so on. Ugelstad et al.,[18] who reported the preparation of monosized magnetic microspheres with micron size, have done the pioneer work in this field. Furusawa et al.[19] investigated a heterocoagulation concept.

Considering the mechanism of different emulsion polymerizations, the miniemulsion polymerization is very suitable for making magnetic polymeric particles and the encapsulation of inorganic particles.[20] One of the characteristic features of the miniemulsion polymerization technique may be an advantageous encapsulation method. Potential advantages include the ability to control the size via formulation of the miniemulsion, direct dispersing the hydrophobic inorganic particles in the monomer phase, the ability to nucleate all the droplets containing inorganic particles, and faster polymerization.[21–23]

*Correspondence to:* A. R. Mahdavian (a.mahdavian@ippi.ac.ir).

Contract grant sponsor: Iran Polymer and Petrochemical Institute (IPPI); contract grant number: 24761129.

To obtain a successful encapsulation, the magnetite aggregates have to be hydrophobized to make them dispersible in hydrophobic monomers such as styrene. A mixture of magnetite particles and styrene was miniemulsified in water, and after polymerization, polymer-encapsulated magnetite particles were obtained.[24] The key to success of using miniemulsion polymerization to prepare a magnetic emulsion is to generate an ultrafine and stable dispersion of magnetic particles in the monomers.[25]

Ultrasonic irradiation has been widely used in chemical industries, such as dispersion, emulsifying, crushing, organic synthesis, and initiating the polymerization of the monomer.[26] Ultrasonically initiated emulsion polymerization has many advantages, such as chemical-free initiation and low reaction temperature. Ultrasonically initiated emulsion polymerization has been employed for preparation of poly (butyl acrylate)/carbon nanotubes,[27] poly (butyl acrylate)/$SiO_2$,[28] poly (butyl methacrylate)/$Al_2O_3$ nanocomposites.[29] Ultrasonically initiated miniemulsion polymerization process in the presence of inorganic nanoparticles has been reported by Wang and coworkers[30] previously. Their investigations were limited to the affecting parameters such as emulsifier, stabilizer, and hydrophobe amounts on the extent of polymerization rate and coagulum percent. The magnetite content in the polymeric phase was 3% (wt %) and nothing was performed on the magnetization, morphologic and particle size distribution in their studies.

Here, the optimized conditions were applied to develop the encapsulation efficiency with regard to morphological studies for obtaining particles with nanometric size. In this work and in continuum to our previous report on preparation of nanocomposite particles with core-shell morphology through emulsion polymerization,[31] chemical initiator-free miniemulsion polymerization has been used to prepare MCPs with styrene and butyl acrylate (BA) as monomers, span 80 as a stabilizer, sodium dodecyl sulfate (SDS) as an ionic surfactant, and hexadecane (HD) as hydrophobic agent.

## EXPERIMENTAL

### Materials

Iron oxide (II, III) nanopowder $\geq$ 98% with spherical shape, 20–30 nm particle size diameter, and surface area $>$ 60 $m^2/g$ from BET test were obtained from Aldrich (Gillingham, UK). Styrene (St) from Merck Chemical (Darmstadt, Germany) (analytical grade) was washed with 5 wt % sodium hydroxide aqueous solution to remove the inhibitor, dried over calcium chloride, and stored at 0°C. BA from Fluka (Buchs, Germany), SDS from Aldrich, oleic acid, HD, and span 80 as a nonionic surfactant from Merck Chemical were used without further purification.

**TABLE I**
**A Typical Recipe Used for the Encapsulation Process**

| Components | Amount (g) | Ratio |
|---|---|---|
| St | 6.24 | 0.06 mol |
| BA | 7.7 | 0.06 mol |
| HD | 0.7 | 5 wt %[a] |
| SDS | 0.42 | 3 wt %[a] |
| Span 80 | 0.39 | 2.5 wt %[a] |
| m-$Fe_3O_4$ | 0.697–2.1 | 5–15 wt %[a] |
| Distillated water | 65–71.5 | 80 wt %[b] |

[a] Based on the total weight of monomers.
[b] Based on the total weight of latex.

### Preparation of surface-modified $Fe_3O_4$ (m-$Fe_3O_4$)

Four grams of $Fe_3O_4$ was dispersed in 70 mL distilled water under ultrasonic irradiation for 5 min, then 1.8 mL oleic acid was added and ultrasonication was continued. Six milliliters of 25 wt % aqueous ammonia solution was added and dispersing was carried on with the aid of ultrasound waves for 5 min. The obtained dispersion was stirred for 120 min and then it was acidified with concentrated HCl (pH = 2–4). The dispersed phase was separated by using ultracentrifuge (3000 rpm), washed with 3 : 1 (v/v) of ethanol : water (once), 1 : 1 (v/v) of ethanol : water (twice), and dried at 50°C for 20 h. Finally 3.85 g of modified $Fe_3O_4$ was obtained.

### Ultrasonically initiated miniemulsion polymerization

Equimolar amounts of St and BA (0.06 mol), definite amount of $Fe_3O_4$, and 0.39 g span 80 (as stabilizer) were premixed through ultrasonication for 5 min at room temperature to reach the optimum dispersion of $Fe_3O_4$ nanoparticles in the monomer phase. HD (0.7 g) was dissolved in the monomer phase and the obtained mixture was added to the water phase containing 0.42 g SDS and a definite amount of double distilled water. The reactor temperature was set at 33°C by using a thermostatic bath, and the polymerization reaction was progressed under $N_2$ atmosphere and ultrasonic irradiation for 90 min. Brownish latex was obtained at the end of polymerization reaction. The conversions in all experiments were around 60–65% relative to the initially added nonvolatile components (including monomers, $Fe_3O_4$, and surfactants amounts). The detailed amounts of ingredients for each sample have been listed in Tables I and II. Polymer films for relating analysis were prepared by drying the latices at room temperature for 2 days and subsequently, drying the cast films in an oven at 45°C for 20 h.

### Characterization methods

The equipment employed in this search was a 20 kHz $\pm$ 500 Hz Ultrasonic generator, SONOPULS

Ultrasonic homogenizer, Model HF-GM 2200 (BANDELIN electronic GmbH and Co. KG, Berlin, Germany) and the probe used was a titanium microtip MS-73 with the diameter 3 mm. The miniemulsion polymerization was performed in a designed set-up according to Figure 1. FTIR spectra were also recorded on a FTIR BRUKER-IFS 48 spectrophotometer (Ettlingen, Germany) using KBr pellets. Thermogravimetric analysis (TGA) was performed on a Perkin–Elmer Pyris (Massachusetts, USA) 1 under $N_2$ atmosphere from room temperature up to 700°C at a heating rate of 20°C/min. Mean particle size was measured by SEMATECH light scattering (Nice, France) with 633 nm wavelength. Size and morphology of the samples were also investigated by scanning electron microscopy (SEM) with XL30 instrument from Philips Co (Almelo, The Netherlands). A drop of the latex was placed on the sample holder and dried under freeze-drying. They were then put under vacuum, flushed with argon (Ar), evacuated, and sputter-coated with gold for SEM analysis. TEM micrographs were taken by a CEM 902A ZEISS transmission electron microscope with an accelerating voltage of 80 keV (Oberkochen, Germany). The samples were diluted up to 20 times (v/v), stained with osmium oxide ($OsO_4$), dropped on a copper grid covered by formvar foil (200 mesh) and dried for TEM analysis. Magnetic properties of the particles were determined by a vibrating-sample magnetometer (VSM); model 155, Princeton Applied Research (New Jersey, USA).

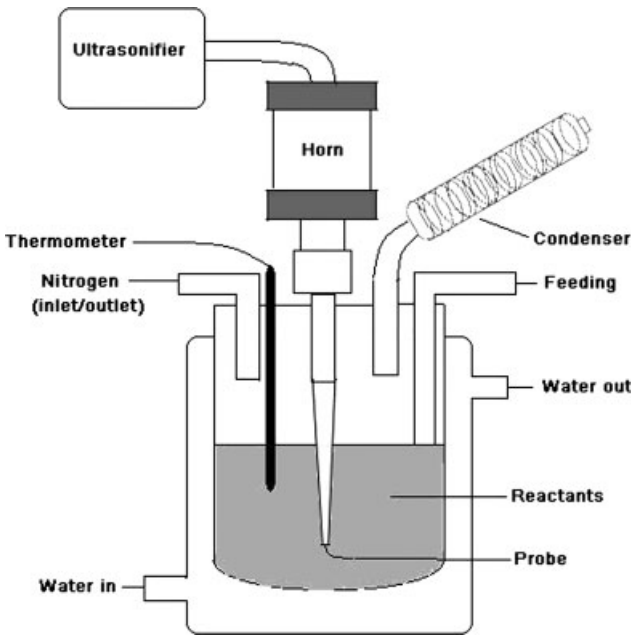


**Figure 1** The designed reactor for ultrasonically initiated miniemulsion polymerization.

## RESULTS AND DISCUSSION

### Surface modification of magnetite nanoparticles

Miniemulsion polymerization is one of the most applicable methods for encapsulation of inorganic nanoparticles by polymeric materials and is still under improvement. $Fe_3O_4$ nanoparticles have large surface area to volume ratio and tend to aggregate for reducing of surface tension. Hence, one of the major problems in preparation of stable ferrofluids is to prevent aggregation process during their synthesis and coating. Double-layer surfactants are usually used for this purpose.[32]

Good encapsulation was achieved during an effective dispersion process. For better dispersion of $Fe_3O_4$ nanoparticles in the oil phase (styrene-butyl acrylate mixture), it was necessary to coat $Fe_3O_4$ nanoparticles' surface with organic compounds such as oleic acid. Here, modification was carried out by ammonium oleate, which was obtained from the *in situ* reaction of oleic acid with ammonia. The modified (oleated) $Fe_3O_4$ (m-$Fe_3O_4$) has more susceptibility for dispersion in the monomer phase.

**TABLE II**
**Several MCPs Prepared with Different Magnetite Content**

| Sample | Amount of m-$Fe_3O_4$ (g) | Magnetite content[a] (wt %) | Coagulation[b] (wt %) |
|---|---|---|---|
| SBF-1 | 0.697 | 5 | 2.6 |
| SBF-2 | 1.05 | 7.5 | 5.3 |
| SBF-3 | 1.4 | 10 | 7.2 |
| SBF-4 | 1.74 | 12.5 | 9.1 |
| SBF-5 | 2.1 | 15 | 9.4 |
| SBu[c] | 0 | 0 | 0 |

[a] [m-$Fe_3O_4$ (g)]/[monomer (g)] × 100.
[b] Relative to the total solid content of the latex.
[c] The blank sample prepared without any m-$Fe_3O_4$.

### Chemical initiator-free miniemulsion polymerization

As a brief comparison between emulsion and miniemulsion polymerization techniques in encapsulation of inorganic nanoparticles, the encapsulating material is dispersed in the monomer phase prior to emulsification in miniemulsion polymerization and this will enhance the efficacy of encapsulation process. In the miniemulsions, however, the presence of a cosurfactant acts to reduce substantially the rate of diffusion of oil from smaller to larger droplets that will cause lower polydispersity of particles size. In these series of miniemulsion polymerization reactions, no chemical initiator was used in the recipes and the free radicals needed for initiation were supplied from the decomposition of surfactant, water,

and monomer molecules by ultrasonic cavitations.[26] Here, the first step is preparation of a successful dispersion of magnetite nanoparticles in the monomer phase. Anionic surfactants such as SDS were unable to produce a stable dispersion and thus nonionic ones were experienced. Some types of Tritons were tested and did not give good results and eventually, span 80 was chosen among several nonionic emulsifiers for preparation of the above stable dispersion. In the next step, the oil phase containing $Fe_3O_4$ nanoparticles was dispersed in the water phase including SDS and HD to form minidroplets. While ultrasonication continued, miniemulsion polymerization was initiated and progressed. As a matter of fact, the local temperature produced by the collapse of the bubbles is estimated to be several hundred to several thousand degrees Kelvin. This is able to split the organic molecules homolitically, to produce free radicals and to induce free radical reactions.

During miniemulsification, monomer droplets containing m-$Fe_3O_4$ are formed in the range of 50–500 nm depending on the SDS/HD ratio,[33] meanwhile this diameter will be 10–20 μm in conventional emulsions. When the ultrasonifier is used to form the miniemulsion, the ultrasonic waves can break up the monomer droplets. It is also notable that the droplet size has inverse proportionality with ultrasonication time and latex particles will follow this trend subsequently.[20] Because of the combined and synergistic effect of surfactant and hydrophobe, monomer droplets are stable enough to prevent diffusion of monomers to the continuous phase. This will cause with respect to the absence of micelles and consequently impossibility of nucleation in the continuous phase.

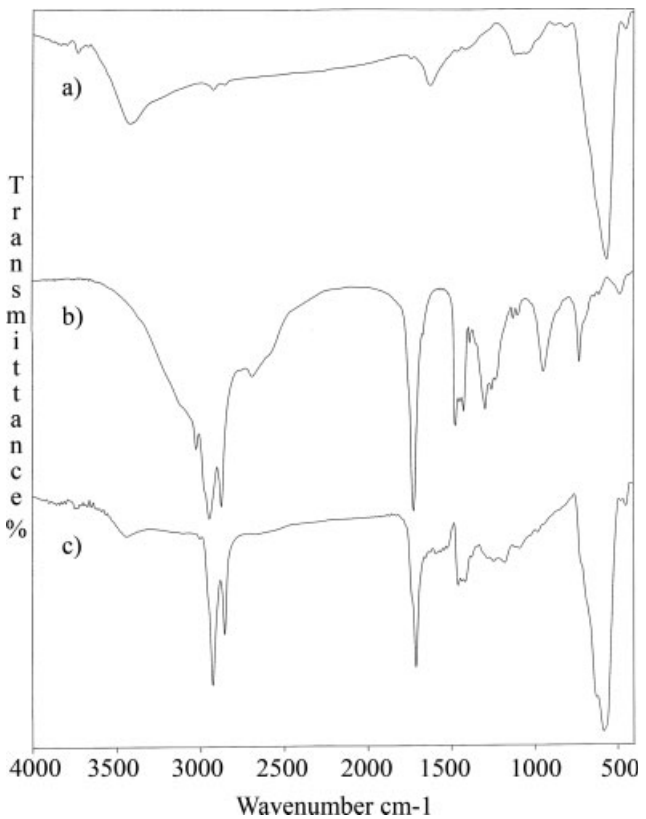


**Figure 2** The FTIR spectra of (a) primary $Fe_3O_4$ nanoparticles, (b) pure oleic acid, and (c) oleic acid-modified magnetite particles (m-$Fe_3O_4$).

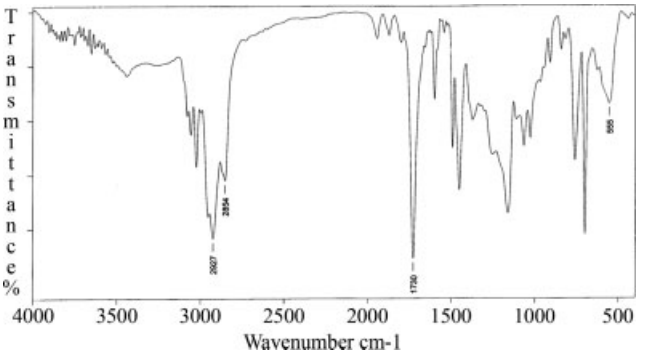


**Figure 3** Typical FTIR spectrum of the prepared magnetic nanocomposite particles.

## FTIR analysis

FTIR spectra were recorded to confirm the structure of oleated $Fe_3O_4$ nanoparticles and also incorporation of magnetite into the St-BA copolymers. Before taking FTIR spectra, the prepared m-$Fe_3O_4$ was washed with plenty of 1 : 3 and 1 : 1 of ethanol: water several times for removal of unreacted oleic acid or ammonium oleate from the precipitated m-$Fe_3O_4$ nanoparticles. Figure 2 shows FTIR spectra of pure $Fe_3O_4$ nanoparticles (a), oleic acid (b), and m-$Fe_3O_4$ nanoparticles (c).

The characteristic peak of magnetite appears at 562 $cm^{-1}$, which corresponds to the bending vibration of Fe—O [Fig. 2(a)]. Those characteristic peaks for oleic acid are at 1709 $cm^{-1}$ relating to C=O stretching bond, 2854 and 2924 $cm^{-1}$ for C—H stretching modes [Fig. 2(b)]. In Figure 2(c), there exist bands of both $Fe_3O_4$ and oleic acid that proves formation of modified $Fe_3O_4$. This means that oleic acid salt has been adsorbed (chemisorbed) on the $Fe_3O_4$ nanoparticle surface.

FTIR spectrum of the obtained MCPs shows the presence of both m-$Fe_3O_4$ and St-BA copolymer (Fig. 3) with respect to the spectrum of styrene-butyl acrylate copolymer.[34]

## Thermal gravimetric analysis of the obtained MCPs

Thermal gravimetric analysis (TGA) was used to investigate the effect of the incorporated m-$Fe_3O_4$ into the polymer phase, on thermal behavior of the

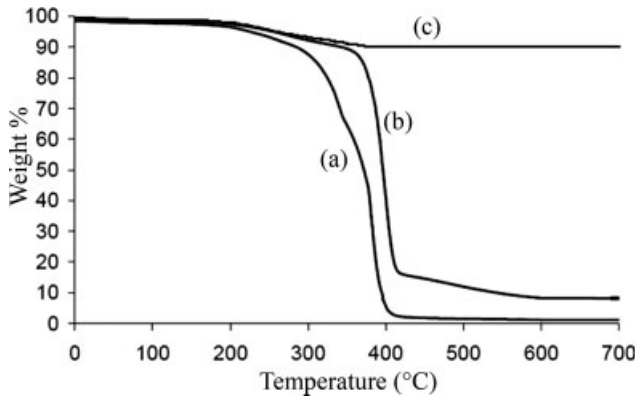


**Figure 4** TGA curves of the blank copolymer [SBu sample] (a), the prepared magnetic nanocomposite particles [SBF-5 sample] (b), and oleic acid-modified magnetite particles (c).

MCPs. The amount of residue at 700°C in TGA thermograms also gives a reasonable estimation of m-$Fe_3O_4$ amount in the polymeric latex particles. TGA thermograms for the SBF-5 sample, the blank sample (SBu) containing St-BA copolymer without any magnetite (produced by the same recipe), and m-$Fe_3O_4$ have been shown in Figure 4. The weight loss in the range of 250–350°C in m-$Fe_3O_4$ is related to the degradation of adsorbed oleic acid to $Fe_3O_4$.

It could be observed that thermal resistance of MCPs is increased through incorporation of magnetite into the polymeric phase. This improvement in the initial decomposition temperature is about 60–80°C (Fig. 4). It is also interesting that a remarkable decomposition or degradation, which occurs at 320°C for SBu sample, could not be found for SBF-5 sample (Fig. 5).

This means that the magnetite has affected thermal degradation phenomena through its effective interaction with the surrounding copolymer and prevents or postpones some degradative processes.

The amount of residue at 700°C for SBF-2 and SBF-5 were 5.5 and 12.2%, respectively, which leads to a good estimation of the encapsulated magnetite in the polymer particles. If there exists any bare m-$Fe_3O_4$ (not encapsulated), they could not maintain their dispersibility and after stopping agitation will precipitate readily due to the high density of the magnetite particles (4.8–5.1 g/mL at 25°C) and its bulk density (0.84 g/mL). Therefore, a macroscopic observation for determination of the extent of encapsulation is to measure the amount of precipitated m-$Fe_3O_4$ at the end of polymerization reaction. It is notable that measurement of the precipitate weight and what is observed from TGA thermograms both conform with each other in determination of the amount of encapsulated m-$Fe_3O_4$ and reveal that the encapsulation process has been performed in about 4–13.5 wt % (magnetite content) for all samples.

### Dynamic light scattering analysis

Particle size distributions of different MCPs of different samples were determined by dynamic light scattering (DLS) technique and have been listed in Table III. It is observable that mean particle size diameter of different MCPs are decreased with increasing the amount of $Fe_3O_4$ in the recipe up to 10% (by weight) and this is the same as the trend reported by Xie et al.[3] By increasing $Fe_3O_4$ amount from 10 to 15%, the particle size is increased in contrast with the above observation (Table III).

The decrease in particle size of the final latex with the increase in m-$Fe_3O_4$ amount comes from the fact that the amount of m-$Fe_3O_4$ has direct proportionality with the number of minidroplets or nucleating loci. The acoustic intensity in liquid mixtures is increased with the increase in the particle numbers[35] and this will affect on fission/fusion process. That is, fission phenomenon, which is generated from ultrasonication causes the decrease in minidroplet size and has priority over fusion process. This will result in overall decrease in the minidroplet size.

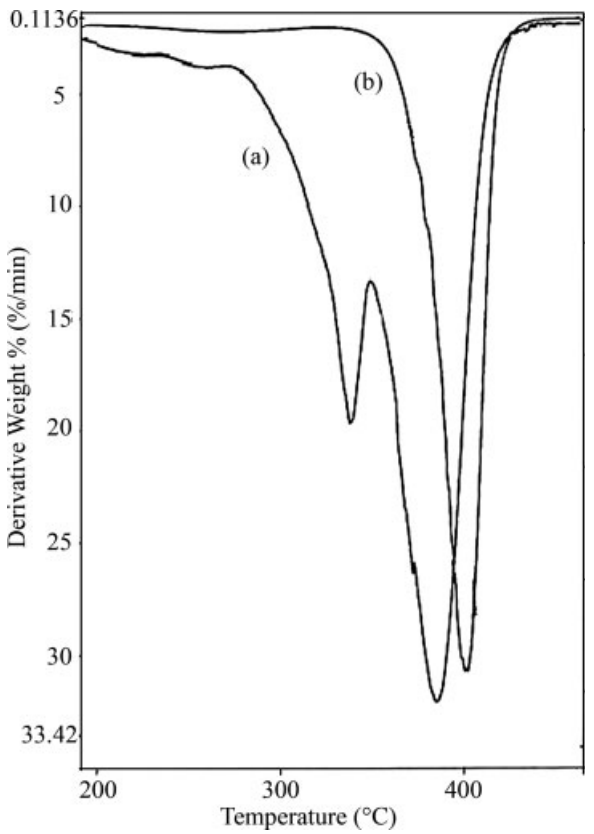


**Figure 5** Differential thermogravimetry (DTG) curves in the 200–500°C for the blank copolymer [SBu] (a) and the prepared magnetic nanocomposite particles [SBF-5 sample] (b).

**TABLE III**
**Mean Particle Size Diameter for Different Samples Obtained from DLS Analysis**

| Sample | Particle diameter (nm) | $\sigma_n$ [a] |
|---|---|---|
| SBU | 103 | 5.17 |
| SBF-1 | 120.6 | 2.44 |
| SBF-2 | 97.2 | 1.7 |
| SBF-3 | 81.1 | 1.91 |
| SBF-4 | 127.4 | 0.98 |
| SBF-5 | 149.9 | 1.28 |

[a] Standard deviation.

The increase in particle size from SBF-3 to SBF-5 probably comes from the absence of optimized conditions for stabilization. The increase in m-$Fe_3O_4$ amount not only results in more particle number but also makes the particles become larger. This means that more m-$Fe_3O_4$ particles would enter into the monomer minidroplets to cause this enlargement. It is worthy noting that the increase in m-$Fe_3O_4$ amount without changing the surfactant concentration makes the particle size enlargement. On the other hand, the significant increase in surfactant concentration causes the droplets to become smaller to such extent that they may not allow easy dispersion of $Fe_3O_4$ particles in the monomer droplets or would push out the previously dispersed ones. It is concluded that the variation in magnetite content should be provided with the change in the recipe to have monodisperse MCPs accordingly. We only changed the magnetite content while keeping all components constant. Of course there is a report on the variation of magnetite content at a constant formulation.[25]

## SEM and TEM analysis

Morphology of the MCPs was studied by scanning and transmission electron microscopy. SEM micrograph of the SBF-5 particles has been shown in Figure 6. It is clear that the particles have spherical shape and their sizes are around 140–160 nm. The smooth surface of the MCPs reveals that no m-$Fe_3O_4$ nanoparticle has been deposited on the shell or surface of the particles and they have been encapsulated by the copolymer. The obtained particle sizes from SEM micrographs also confirm the data from DLS analysis (Table III).

Transmission electron microscopy was applied to investigate the core-shell morphology of the MCPs (Fig. 7). It could be observed that the magnetite particles have been placed as dark phase in the core and St-BA copolymer as light phase in the shell. It is evident that the encapsulation of magnetite particles has been performed and the core-shell morphology has been obtained successively. This morphology is

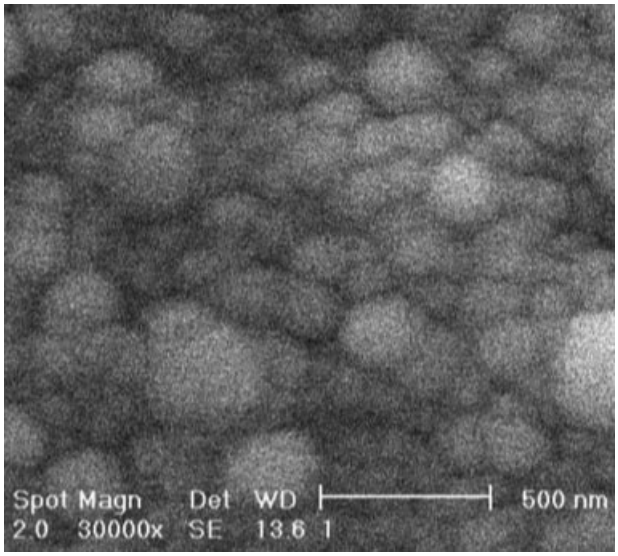


**Figure 6** SEM micrograph of the obtained MCPs from SBF-5 sample.

the result of nucleation in the monomer droplets that has been discussed before.[33] Also TEM micrographs confirm the occurrence of dispersion of magnetite in the polymeric phase at nanoscale.

It should be noted that no free m-$Fe_3O_4$ was found in the latex according to the TEM micrographs. This is due to the good dispersion of hydrophobic m-$Fe_3O_4$ in the monomer phase. Then monomer droplets containing m-$Fe_3O_4$ nanoparticles have been dispersed in the aqueous phase and stabilized

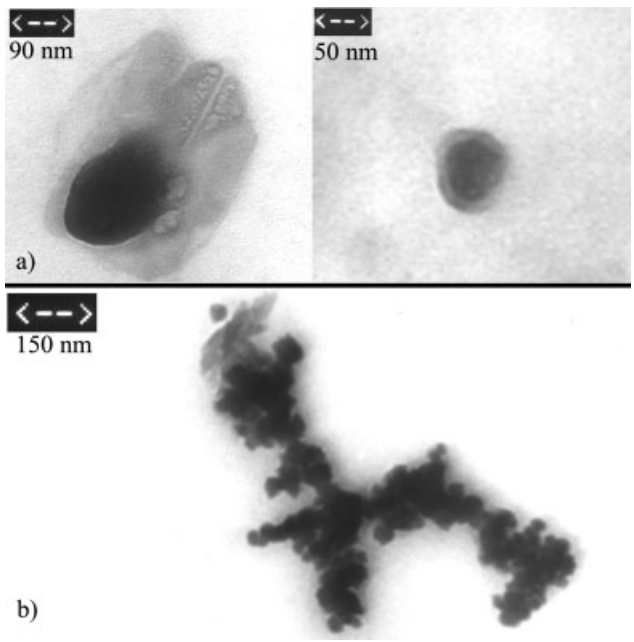


**Figure 7** TEM micrographs of the prepared core-shell MCPs from SBF-5 sample. (a) Single particle and (b) aggregate of the particles.

by surfactant (SDS) and cosurfactant (HD). The migration of m-$Fe_3O_4$ from stabilized minidroplets occurs hardly and those that come out could not maintain their dispersibility and will aggregate and precipitate during progress of miniemulsion polymerization.

### Magnetic properties of the prepared MCPs

The study of variation of magnetization with applied magnetic field gives useful information about magnetic properties of the magnetic polymeric particles. Magnetic hysteresis loop is the characteristic of such magnetic particles. Here, vibrating sample magnetometer (VSM) was used for studying the magnetization of prepared MCPs. The result of VSM analysis shows the response ability of magnetic materials toward external magnetic fields, in which their characteristic parameters are saturation magnetization ($M_s$), coercive force ($H_c$), and remanence magnetization ($M_r$).

Figure 8 shows a typical magnetization variation of m-$Fe_3O_4$. The variation has been given in Figure 9 for SBF-5 sample. These two figures show that the magnetic hysteresis loops for m-$Fe_3O_4$ and prepared MCPs (SBF-5) are both S-shape and almost similar. The saturation magnetization of the prepared MCPs for SBF-5 sample was found to be 8.22 emu/g ($H$ = 10 KOe), the remanence magnetization, $M_r$ = 1.93 emu/g, and the coercive force, $H_c$ = 69.1 Oe (while it is 0.063–12.6 Oe for soft magnetic materials). Also for this sample at $H$ = 1250 Oe, the magnetization was found to be equal to 6.95 emu/g.

The saturation magnetization of SBF-5 sample (8.22 emu/g) interprets that the particles have got magnetic response to a certain extent. The comparison between obtained saturation magnetizations from hysteresis loops of SBF-5 (8.22 emu/g) and m-$Fe_3O_4$ (58.71 emu/g) reveals that the magnetite content in SBF-5 is about 14 wt %, which is in accordance with the TGA data and the initial added magnetite in the recipe.

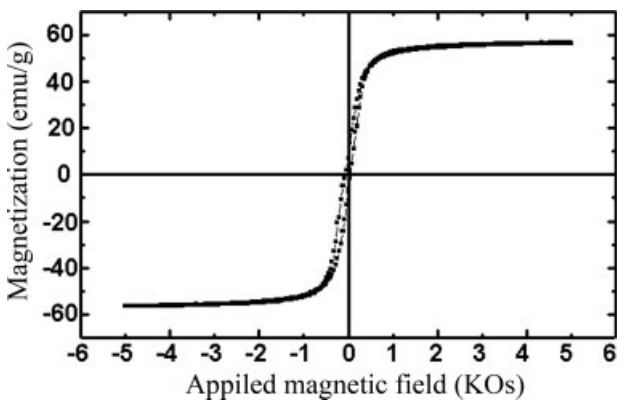


**Figure 8** Magnetic hysteresis loop of magnetite particles modified with oleic acid (m-$Fe_3O_4$).

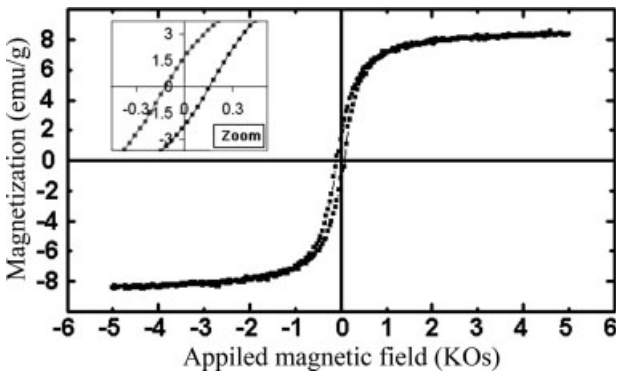


**Figure 9** Magnetic hysteresis loop of the obtained MCPs of SBF-5 sample.

## CONCLUSIONS

Here, colloidal particles were prepared with magnetic properties through chemical initiator-free miniemulsion polymerization of styrene and BA. The polymerization reaction was initiated and progressed by the immersed probe ultrasonic irradiation to obtain 81–150 nm core-shell nanocomposite particles, in which modified $Fe_3O_4$ nanoparticles have been encapsulated as the core. MCPs were obtained in the presence of 3 wt % SDS as surfactant, 2.5 wt % span 80 as stabilizer, and 5 wt % HD as hydrophobic agent. Obtaining a stable colloidal dispersion at the end of reaction is a macroscopic evaluation of the progress of encapsulation process. Characterization of the products by FTIR spectroscopy showed the progress of reaction at each step. Particle size diameter in the latex form up to 150 nm was measured by DLS analysis and their core-shell morphologies were confirmed by SEM and TEM micrographs. TGA and magnetometry of the polymeric films revealed that 14 wt % of magnetite has been incorporated into the polymeric phase, and the corresponding magnetization behavior of the films was studied.

Helpful assistance of Mr. Hashemi for taking TEM micrographs from Faculty of Science, University of Tehran is greatly acknowledged.

### References

1. Liu, X.; Guan, Y.; Ma, Z.; Liu, H. Langmuir 2004, 20, 10278.
2. Caruso, F.; Susha, A. S.; Giersig, M.; Möhwald, H. Adv Mater 1999, 11, 950.
3. Xie, G.; Zhang, Q.; Luo, Z.; Wu, M.; Li, T. J Appl Polym Sci 2003, 87, 1733.
4. Sieben, S.; Bergemann, C.; Lubbe, A.; Brockmann, B.; Rescheleit, D. J Magn Magn Mater 2001, 225, 175.
5. Tanyolac, D.; Zdural, A. R. J Appl Polym Sci 2001, 80, 707.
6. Pyle, B. H.; Broadaway, S. C.; McFeters, G. A. Appl Environ Microbiol 1999, 65, 1966.

7. Avital, I.; Inderbitzin, D.; Aoki, T.; Tyan, D. B.; Cohen, A. H.; Ferraresso, C.; Rozga, J.; Arnaout, W. S.; Demetriou, A. A. Biochem Biophys Res Commun 2001, 288, 156.
8. Cumbal, L.; Greenleaf, J.; Leun, D.; SenGupta, A. K. React Funct Polym 2003, 54, 167.
9. Lee, Y.; Rho, J.; Jung, B. J Appl Polym Sci 2003, 89, 2058.
10. Schmidt, A. M. Macromol Rapid Commun 2005, 26, 93.
11. Yanase, N.; Noguchi, H.; Asakura, H.; Suzuta, T. J Appl Polym Sci 1993, 50, 765.
12. Wang, P. C.; Chiu, W. Y.; Lee, C. F.; Young, T. H. J Polym Sci Polym Chem 2004, 42, 5695.
13. Wormuth, K. J Colloid Interface Sci 2001, 241, 366.
14. Deng, Y.; Wang, L.; Yang, W.; Fu, S.; Elaïssari, A. J Magn Magn Mater 2003, 257, 69.
15. Hoffmann, D.; Landfester, K.; Antonietti, M. Magnetohydrodynamics 2001, 37, 217.
16. Horak, D.; Benedyk, N. J Polym Sci Part A: Polym Chem 2004, 42, 5827.
17. Zaitsev, V. S.; Filimonov, D. S.; Presnyakov, I. A.; Gambino, R. J.; Chu, B. J Colloid Interface Sci 1999, 212, 49.
18. Ugelstad, J.; Berge, A.; Ellingsen, T.; Schmid, R.; Nilsen, T.-N.; Mork, P. C.; Stenstad, P.; Hornes, E.; Olsvik, O. Prog Polym Sci 1992, 17, 87.
19. Furusawa, K.; Nagashima, K.; Anzai, C. Colloid Polym Sci 1994, 272, 1104.
20. Xu, Z. Z.; Wang, C. C.; Yang, W. L.; Deng, Y. H.; Fu, S. K. J Magn Magn Mater 2004, 277, 136.
21. Asua, J. M. Prog Polym Sci 2002, 27, 1283.
22. Landfester, K.; Bochthhold, N.; Foster, S.; Antinietti, M. Macromol Rapid Commun 1999, 20, 81.
23. Csetneki, I.; Faix, M. K.; Szilagyi, A.; Kovacs, A. L.; Nemeth, Z.; Zrinyi, M. J Polym Sci Polym Chem 2004, 42, 4802.
24. Ramirez, L. P.; Landfester, K. Macromol Chem Phys 2003, 204, 22.
25. Lu, S.; Forcada, J. J Polym Sci Part A: Polym Chem 2006, 44, 4187.
26. Feng, N.; Li, H. M. Sonochemistry and its Applications; Anhui Science and Technology Publishing House: Hefei, 1992.
27. Xia, H. S.; Wang, Q.; Qiu, G. H. Chem Mater 2003, 15, 3879.
28. Xia, H. S.; Zhang, C. H.; Wang, Q. J Appl Polym Sci 2001, 80, 1130.
29. Liao, Y. Q.; Wang, Q.; Xia, H. S. Polym Int 2001, 50, 207.
30. Qiu, G. H.; Wang, Q.; Wang, C.; Lau, W.; Guo, Y. Polym Int 2006, 55, 265.
31. Mahdavian, A. R.; Ashjari, M.; Bayat-Makoo, A. Eur Polym J 2007, 43, 336.
32. Wooding, A.; Kilner, M.; Lambrick, D. B. J Colloid Interface Sci 1991, 144, 236.
33. Antonietti, M.; Landfester, K. Prog Polym Sci 2002, 27, 689.
34. Hummel, D. O.; Scholl, F. Atlas of Polymer and Plastic Analysis, Part a/I; Carl Hanser Verlag: München, 1990; Vol. 2, p 384.
35. Tuziuti, T.; Yasui, K.; Iida, Y.; Taoda, H.; Koda, S. Ultrasonics 2004, 42, 597.